Article

Geliboluols A–D: Kaurane-Type Diterpenoids from the Marine-Derived Rare Actinomycete *Actinomadura geliboluensis*

Chang-Su Heo [1,2], Jong Soon Kang [3], Jeong-Wook Yang [3], Min Ah Lee [1,4], Hwa-Sun Lee [1,4], Chang Hwan Kim [5] and Hee Jae Shin [1,2,*]

[1] Marine Natural Products Chemistry Laboratory, Korea Institute of Ocean Science and Technology, 385 Haeyang-ro, Busan 49111, Republic of Korea; science30@kiost.ac.kr (C.-S.H.); minah@kiost.ac.kr (M.A.L.); hwasunlee@kiost.ac.kr (H.-S.L.)

[2] Department of Marine Technology and Convergence Engineering, University of Science and Technology (UST), 217 Gajungro, Daejeon 34113, Republic of Korea

[3] Laboratory Animal Resource Center, Korea Research Institute of Bioscience and Biotechnology, 30 Yeongudanjiro, Cheongju 28116, Republic of Korea; kanjon@kribb.re.kr (J.S.K.); z7v8@kribb.re.kr (J.-W.Y.)

[4] Department of Chemistry, Pukyong National University, 45 Yongso-ro, Busan 48513, Republic of Korea

[5] Dokdo Research Center, Korea Institute of Ocean Science and Technology, Uljin 36315, Republic of Korea; kimch@kiost.ac.kr

* Correspondence: shinhj@kiost.ac.kr; Tel.: +82-51-664-3341; Fax: +82-51-664-3340

Abstract: Four new kaurane-type diterpenoids, geliboluols A–D (**1–4**), along with one known analog (**5**), were isolated from the culture broth of the marine-derived rare actinomycete *Actinomadura geliboluensis*. The structures of compounds **1–4** were determined by spectroscopic analysis (HR-ESIMS, 1D, and 2D NMR), the MPA method, and by comparing their optical rotation values with those in the literature. The new compounds were evaluated for their cytotoxicity against seven blood cancer cell lines by a CellTiter-Glo (CTG) assay and six solid cancer cell lines by a sulforhodamine B (SRB) assay. Among the new compounds, compound **4** exhibited moderate cytotoxic activity against some blood cancer cell lines, with GI_{50} values ranging from 2.59 to 19.64 μM, and against solid cancer cell lines with GI_{50} values ranging from 4.34 to 7.23 μM.

Keywords: *Actinomadura geliboluensis*; kaurane; diterpenoids; cytotoxicity; geliboluol

1. Introduction

Diterpenoids, a class of secondary metabolites, are comprised of four isoprene units with twenty carbons. Such diterpenoids are classified as labdanes, pimaranes, kauranes, trachylobane, and so on, depending on the type of cyclization and the number of rings [1,2]. Among diterpenoids, kauranes are tetracyclic diterpenes with four carbon ring moieties [3]. Their structural scaffolds typically consist of a perhydrophenantrene moiety with rings A, B, as well as C (Figure 1), and a cyclopentane moiety with ring D, which is fused at the C-8 and C-13 positions [2]. Depending on the inversion of stereocenters, enantiomers are distinguished into two types, kauranes and *ent*-kauranes. The majority of enantiomers belong to *ent*-kauranes and generally, they have negative values of optical rotation [2]. Most kaurane diterpenoids are discovered in plant sources such as the Lamiaceae family, as well as Asteraceae, Annonaceae, and Euphorbiaceae [3,4]. They are known to be involved in the protective functions of plants that produce them [5,6]. Additionally, their broad biological activities have been reported, including antiparasitic, antifungal, antibacterial, antitumor, anti-inflammatory, and antiviral activities in previous research [4,7–12].
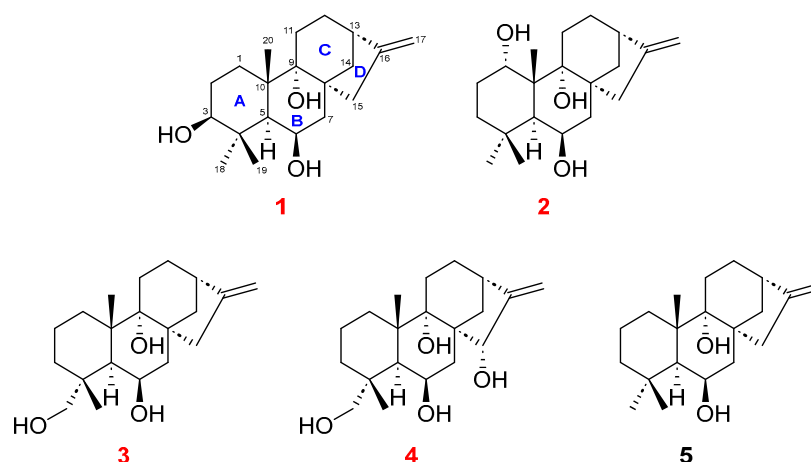
Figure 1. Structures of compounds **1**–**5** isolated from *Actinomadura geliboluensis* 238DD-017.

Actinobacteria are well-known as an abundant source of secondary metabolites in explorations of novel medicines [13]. They are not only contributors to antibiotic production, such as streptomycin and kanamycin, but are also producers of anti-cancer compounds such as doxorubicin and salinosporamide [14,15]. Among them, *Actinomadura*, a genus of Actinomycetes, has been relatively less-studied than the genus *Streptomyces*, which is common in Actinobacteria. To date, over 70 species of *Actinomadura* have been identified and more than 230 compounds derived from those species have been reported for their unique structures, along with their various bioactivities [16–18]. Previous molecular biology studies of the *Actinomadura* genus found that more than 30 or 40 putative biosynthetic gene clusters are located on their genomes [19–21], suggesting that most of these are expected to be involved in undiscovered metabolites to date. Therefore, the genus *Actinomadura* has untapped potential in the discovery of novel therapeutic agents [22] and is one of the notable sources of new compounds to explore.

As part of our continuous search for new secondary metabolites from marine microorganisms, an actinobacterial strain was isolated from a sediment sample collected offshore from Dokdo, Republic of Korea. The strain was identified as *Actinomadura geliboluensis* 238DD-017 by 16S rRNA gene sequence analysis. *A. geliboluensis* was first isolated in 2012 in Gelibolu, Canakkale, Turkey [23], and only a few secondary metabolites, such as nomimicins, have been reported from this strain [24]. These facts prompted us to culture this rare strain, and we found the crude extract of the culture broth afforded cytotoxic activity against cancer cell lines. Thus, further study was performed to identify bioactive secondary metabolites produced by the strain. As a result, five kaurane-type diterpenoids, including four new (**1**–**4**) and one known (**5**) derivatives (Figure 1), were isolated from the strain. In this report, the isolation, purification, structure determination, and evaluation of the antimicrobial and cytotoxic activities of the compounds are presented.

2. Results

Compound **1** was isolated as a reddish powder. Its molecular formula was determined as $C_{20}H_{32}O_3$, based on a high-resolution electrospray ionization mass spectrometry (HRESIMS) peak at m/z 343.2239 [M + Na]$^+$ (calcd for $C_{20}H_{32}O_3Na$, 343.2244), requiring an index of hydrogen deficiency of five. The ^1H NMR data (Table 1) showed signals of two exomethylenes at δ_H 4.73 (s, H-17a) and 4.77 (s, H-17b), two oxymethines at δ_H 4.35 (dd, J = 5.0, 2.6 Hz, H-6) and 3.07 (dd, J = 11.7, 4.3 Hz, H-3), fourteen methylenes at δ_H 1.32–2.86, two methines at δ_H 2.59 (overlapped, H-13) and 1.34 (overlapped, H-5), and three methyl groups at δ_H 1.05–1.51. The ^{13}C NMR data (Table 1) and heteronuclear single-quantum coherence (HSQC) NMR data revealed the presence of two olefinic carbons at δ_C 156.6 (C-16)

and 103.0 (C-17), one oxygenated quaternary carbon at δ_C 79.1 (C-9), two oxymethines at δ_C 79.8 (C-3) and 68.7 (C-6), two methines at δ_C 49.5 (C-5) and 44.5 (C-13), three quaternary carbons at δ_C 48.4 (C-8), 44.6 (C-10), and 40.7 (C-4), seven methylenes at δ_C 28.2–45.5, and three methyls at δ_C 28.8 (C-18), 21.8 (C-20), and 17.8 (C-19).

Table 1. ^{1}H (600 MHz) and ^{13}C NMR (150 MHz) data for compounds **1–4** in CD$_3$OD.

No	1		2		3		4	
	δ_H, Mult (*J* in Hz)	δ_C, Type	δ_H, Mult (*J* in Hz)	δ_C, Type	δ_H, Mult (*J* in Hz)	δ_C, Type	δ_H, Mult (*J* in Hz)	δ_C, Type
1a	1.39, ol	33.5, CH$_2$	3.94, t (2.5)	75.4, CH	1.38, ol	35.0, CH$_2$	1.28, ol	33.4, CH$_2$
1b	1.88, td (13.4, 3.9)				1.72 dd (12.6, 3.0)		1.68, ol	
2a	1.59, m	28.2, CH$_2$	1.41, m	28.2, CH$_2$	1.50, m	19.3, CH$_2$	1.48, m	19.2, CH$_2$
2b	1.75, m		2.17, m		1.80, m		1.79, m	
3a	3.07, dd (11.7, 4.3)	79.8, CH	1.03, ddd (13.0, 3.4, 3.3)	37.6, CH$_2$	1.14, ol	38.2, CH$_2$	1.11, dd (12.3, 3.8)	38.1, CH$_2$
3b			1.78, ol		1.46, dd (13.1, 4.0)		1.46, ol	
4		40.7, C		35.1, C		39.7, C		39.6, C
5	1.34, ol	49.5, CH	1.89, d (2.3)	45.8, CH	1.78, ol	44.0, CH	2.02, d (1.9)	43.8, CH
6	4.35, dd (5.0, 2.6)	68.7, CH	4.40, dd (5.6, 3.0)	68.8, CH	4.24, dd (5.0, 2.6)	68.5, CH	4.35, dd (4.7, 2.5)	68.7, CH
7a	1.33, ol	45.3, CH$_2$	1.29, ol	45.0, CH$_2$	1.29, ol	45.0, CH$_2$	1.22, ol	43.6, CH$_2$
7b	2.04, dd (14.2, 3.2)		2.17, dd (14.1, 3.2)		2.08, dd (14.2, 3.2)		2.50, dd (13.9, 3.1)	
8		48.4, C		47.9, C		48.5, C		47.4, C
9		79.1, C		81.5, C		79.2, C		82.0, C
10		44.6, C		46.5, C		44.6, C		45.5, C
11a	1.32, ol	29.7, CH$_2$	1.57, ol	30.9, CH$_2$	1.32, ol	29.6, CH$_2$	1.56, m	31.1, CH$_2$
11b	1.97, dd (14.5, 5.6)		2.12, m		1.98, dd (14.8, 5.5)		2.10, dd (14.8, 5.5)	
12a	1.55, m	35.7, CH$_2$	1.59, m	35.8, CH$_2$	1.55, m	35.7, CH$_2$	1.65, m	36.8, CH$_2$
12b	1.79, m		1.80, m		1.79, m		1.83, m	
13	2.59, ol	44.5, CH	2.59, ol	44.6, CH	2.58, ol	44.8, CH	2.61, ol	41.0, CH
14a	1.38, ol	43.3, CH$_2$	1.35, dd (12.7, 4.8)	42.8, CH$_2$	1.37, ol	43.4, CH$_2$	1.23, ol	39.1, CH$_2$
14b	2.60, ol		2.59, ol		2.62, dd (12.6, 2.8)		2.60, ol	
15a	1.70, d (17.2)	45.5, CH$_2$	1.64, d (17.3)	44.9, CH$_2$	1.68, d (16.7)	45.7, CH$_2$	3.90, t (2.62)	86.7, CH
15b	2.86, d (17.2)		2.84, d (17.3)		2.89, d (16.7)			
16		156.6, C		156.4, C		156.8, C		157.6, C
17a	4.73, s	103.0, CH$_2$	4.73, s	103.0, CH$_2$	4.72, s	102.9, CH$_2$	4.97, s	104.8, CH$_2$
17b	4.77, s		4.78, s		4.78, s		5.07, s	
18a	1.05, s	28.8, CH$_3$	1.01, s	34.2, CH$_3$	3.10, d (11.0)	72.6, CH$_2$	3.10, d (11.1)	72.5, CH$_2$
18b					3.53, d (11.0)		3.54, d (11.1)	
19	1.17, s	17.8, CH$_3$	1.26, s	24.9, CH$_3$	1.14, s	20.4, CH$_3$	1.13, s	20.4, CH$_3$
20	1.51, s	21.8, CH$_3$	1.52, s	22.4, CH$_3$	1.55, s	22.1, CH$_3$	1.53, s	21.7, CH$_3$

In this table, "ol" means overlapped.

The planar structure of **1** was revealed by detailed analyses of ^{1}H-^{1}H correlation spectroscopy (COSY) and heteronuclear multiple-bond correlation (HMBC) NMR data (Figure 2). The ^{1}H-^{1}H COSY spectrum exhibited the following three spin systems: H$_2$-1/H$_2$-2/H-3, H-6/H$_2$-7, and H$_2$-11/H$_2$-12/H-13. The HMBC correlations from H$_3$-18 to C-3, C-4, C-5, and C-19 and from H$_3$-20 to C-1, C-5, and C-10 confirmed the structure of ring A. The HMBC correlations from H-6 to C-8 and C10 and from H$_3$-20 to C-9 established a decalin system of ring B, which was fused with ring A at C-5 and C-10. In addition, the HMBC correlations from H$_2$-11 to C-8 and C-9, from H$_2$-15 to C-8, C-9, and C-14, from H$_2$-14 to C-12, and from H$_2$-17 to C-13, C-15, and C-16 elucidated the structure of a tetracyclic diterpenoid with a 6/6/6/5 ring system, including ring C and ring D. Thus, the gross structure of **1** was determined, as shown in Figure 2.

The relative configuration of **1** was elucidated by the analysis of nuclear Overhauser effect spectroscopy (NOESY) data (Figure 2). The NOESY correlations of H-3 (δ_H 3.07) with H-5 (δ_H 1.34) and H$_3$-18 (δ_H 1.05) and of H-6 (δ_H 4.35) with H$_3$-18 (δ_H 1.05) indicated these protons have an α-orientation, while the NOESY correlations of H$_3$-19 (δ_H 1.17) with H$_3$-20 (δ_H 1.51) suggested the β-orientation of these protons, and the A/B ring junction was a *trans*-configuration. The NOESY correlations of H$_3$-20 with H$_b$-11 (δ_H 1.97) and H$_b$-14 (δ_H 2.60) indicated that they were cofacial and the B/C ring junction was a *cis*-configuration.

Therefore, the relative configuration of chiral centers at C-3, C-5, C-6, C-8, C-9, C-10, and C-13 were identified as 3*S**, 5*S**, 6*R**, 8*R**, 9*R**, 10*S**, and 13*S**.
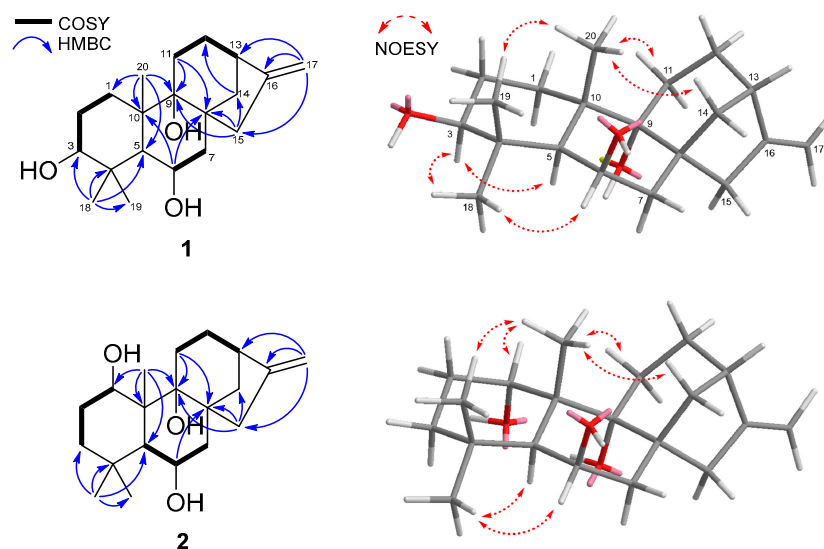

Figure 2. Key COSY, HMBC, and NOESY correlations of compounds **1** and **2**.

The absolute configuration of compound **1** was determined based on its optical rotation value and the MPA method. According to the literature, positive optical rotation values are characteristic of kaurane-type diterpenoids [25,26]. On the contrary, negative optical rotation values of kauranes are usually observed in the *ent*-kaurane-type [2,27–30]. While the majority of kaurane diterpenoids reported to date are on the *ent*-kaurane type [31], unexpectedly, the experimental optical rotation value of **1** was positive ($[\alpha]_D^{25}$ +37.8, *c* 0.1, MeOH) and was consistent with the kaurane type. Therefore, its absolute configuration was reconfirmed by MPA esterification procedures. By comparing ^{1}H NMR data of (*R*)- and (*S*)-MPA esters of **1** (**1a** and **1b**, Figure 3), the absolute configuration of the chiral center at C-3 was identified as 3*S*. Consequently, the absolute configuration of **1** was confirmed as 3*S*, 5*S*, 6*R*, 8*R*, 9*R*, 10*S*, and 13*S*, and **1** was named geliboluol A.
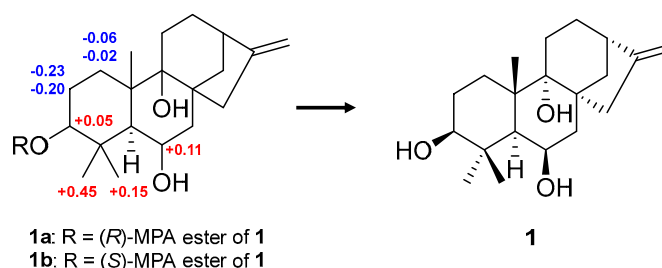

1a: R = (*R*)-MPA ester of **1**
1b: R = (*S*)-MPA ester of **1**

Figure 3. $\Delta\delta_H$ values (in ppm) = $\delta_R - \delta_S$ obtained for (*R*)- and (*S*)-MPA esters of compound **1**. Data were measured in CD$_3$OD.

Compound **2** was isolated as a white powder. Its molecular formula of C$_{20}$H$_{32}$O$_3$ was confirmed based on the HRESIMS peak at *m/z* 319.2273 [M − H]$^-$ (calcd for C$_{20}$H$_{31}$O$_3$, 319.2279), indicating that it was identical to that of **1**. The ^{1}H and ^{13}C NMR spectra of **2** were similar to those of **1**, except for chemical shifts in **2** at C-1 (δ_H 3.94/δ_C 75.4 for **2** and δ_H 1.39, 1.88/δ_C 33.5 for **1**) and C-3 (δ_H 1.03, 1.78/δ_C 37.6 for **2** and δ_H 3.07/δ_C 79.8 for **1**). Comparing the chemical shifts of **2** with those of **1** suggested that the structure of **2** was similar to that of **1**, with a different position for an hydroxy group. Through detailed analysis of the HSQC, COSY, and HMBC data, the hydroxy group of **2** was assigned at C-1 and the planar structure was determined as depicted in Figure 2. The relative configuration

of **2** was confirmed by the interpretation of the NOESY data. The NOESY correlations of **2** were similar to those of **1** and the β-orientation of H-1 was established (Figure 2), revealing the relative configuration of **2** as 1*S**, 5*S**, 6*R**, 8*R**, 9*R**, 10*R**, and 13*S**. The positive optical rotation value of **2** ($[\alpha]_D^{25}$ +29.9, *c* 0.1, MeOH) indicated that **2** is also a kaurane-type diterpenoid. Therefore, the absolute configuration of **2** was elucidated as 1*S*, 5*S*, 6*R*, 8*R*, 9*R*, 10*R*, and 13*S* and given the name geliboluol B.

Compound **3** was isolated as a white powder. Its molecular formula of $C_{20}H_{32}O_3$ was determined based on the HRESIMS peak at *m/z* 343.2229 [M + Na]$^+$ (calcd for $C_{20}H_{32}O_3Na$, 343.2227), revealing that it was consistent with those of **1** and **2**. The ^1H and ^{13}C NMR data of **3** resembled those of **1**, except for the absence of a singlet methyl signal at the C-18 position (δ_H 3.10, 3.53/δ_C 34.2 for **3** and δ_H 1.05/δ_C 28.8 for **1**). Accordingly, it was suggested that the methyl group at C-18 in **1** was changed to an oxygenated methylene in **3**. Further detailed analysis of the HSQC, COSY, and HMBC data confirmed the planar structure of **3** (Figure 4) and the interpretation of NOESY data elucidated the relative structure as 4*R**, 5*S**, 6*R**, 8*R**, 9*R**, 10*S**, and 13*S**, as depicted in Figure 4. The optical rotation value of **3** was positive ($[\alpha]_D^{25}$ +43.5, *c* 0.1, MeOH), and thus the absolute configuration was confirmed as 4*R*, 5*S*, 6*R*, 8*R*, 9*R*, 10*S*, and 13*S*, and **3** was named geliboluol C.
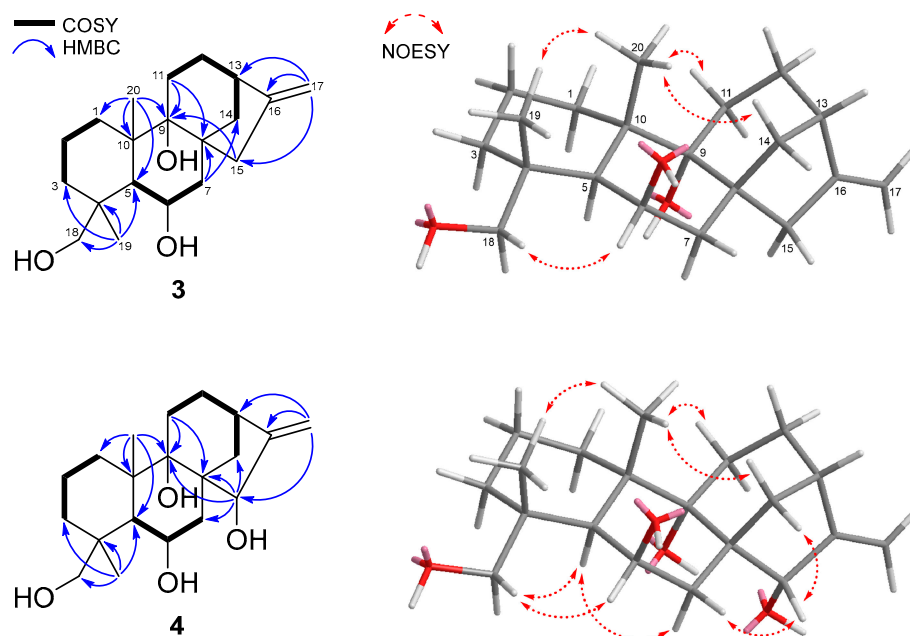

Figure 4. Key COSY, HMBC, and NOESY correlations of compounds **3** and **4**.

Compound **4** was isolated as a white powder with a molecular formula of $C_{20}H_{32}O_4$, as determined by the HRESIMS peak at *m/z* 359.2187 [M + Na]$^+$ (calcd for $C_{20}H_{32}O_4Na$, 359.2193), suggesting the presence of one more oxygen atom in **4** compared to **3**. The ^1H and ^{13}C NMR data of **4** were similar to those of **3**, indicating that the structure of **4** was similar to that of **3**. The only difference was an additional oxymethine signal in **4** at the C-15 position (δ_H 3.90/δ_C 86.7 for **4**, and δ_H 1.68, 2.89/δ_C 45.7 for **3**). The interpretation of 2D NMR data (HSQC, COSY, and HMBC) revealed the planar structure of **4**. The methylene at the C-15 position of **3** was changed to an oxygenated methine in **4**, as shown in Figure 4. The detailed analysis of the NOESY data established the relative structure of **4** (Figure 4). The NOESY correlations of H-15 (δ_H 3.90) with H$_a$-14 (δ_H 1.23) and H$_a$-7 (δ_H 1.22) indicated that they were cofacial, and therefore, the β-orientation of H-15 was confirmed. The absolute configuration of **4** was determined as 4*R*, 5*S*, 6*R*, 8*S*, 9*S*, 10*S*, 13*S*, and 15*S* based on its positive optical rotation value ($[\alpha]_D^{25}$ +59.9, *c* 0.1, MeOH) and given the name geliboluol D.

Bioactivities

Compounds **1–5** were evaluated for their cytotoxicity against seven blood cancer cell lines, the most common cancer types in Korea, along with a normal cell line: HL-60 (acute myelogenous leukemia, AML), Raji (Burkitt's lymphoma), WSU-DLCL2 (diffuse large B-cell lymphoma, DLBCL), NALM6 C. G5 (B-cell acute lymphocytic leukemia, B-ALL), K562 (chronic myelogenous leukemia, CML), RPMI-8402 (T-cell acute lymphocytic leukemia, T-ALL), U266 (multiple myeloma), and RPMI-1788 (B lymphocytes, normal cell line). Compounds **4** and **5** exhibited cytotoxic activity against blood cancer cell lines with GI_{50} values ranging from 2.59 to 22.50 μM (Table 2), while other compounds did not show cytotoxicity against standard cell lines (GI_{50}: >30 μM).

Table 2. Growth inhibition 50% (GI_{50}, μM) values of compounds **1–5** against blood cancer cell lines.

Cell Lines Compounds	HL-60	Raji	WSU-DLCL2	NALM6 C. G5	K562	RPMI-8402	U266	RPMI-1788
1	>30	>30	>30	>30	>30	>30	>30	>30
2	>30	>30	>30	>30	>30	>30	>30	>30
3	>30	>30	>30	>30	>30	>30	>30	>30
4	11.21	2.73	3.48	2.59	19.64	8.51	>30	4.52
5	16.42	4.58	5.93	7.34	11.90	11.09	22.50	9.56
Doxorubicin	0.029	0.014	0.008	0.007	0.094	0.035	0.112	0.012

Doxorubicin is used as a positive control.

Compounds **1–5** were further evaluated for their cytotoxicity against six solid cancer cell lines and a normal cell line: ACHN (renal), MDA-MB-231 (breast), PC-3 (prostate), NUGC-3 (stomach), NCI-H23 (lung), HCT-15 (colon), and MRC-9 (lung fibroblast, normal cell line). Only compound **4** showed cytotoxicity against the six solid cancer cell lines or the normal cell line with GI_{50} values ranging from 4.34 to 7.23 μM (Table 3), while other compounds did not (GI_{50}: >30 μM). When comparing GI_{50} values of **4** with those of the previous studies [10,32], our result displayed a similar tendency. It is noteworthy that **5** has more selective activity against blood cancer cell lines than **4**. Additionally, compounds **1–5** were evaluated for their antimicrobial properties by applying the broth microdilution method, described by the Clinical and Laboratory Standards Institute [33], against three Gram-positive bacteria, *Bacillus subtilis* (KCTC 1021), *Micrococcus luteus* (KCTC 1915), and *Staphylococcus aureus* (KCTC 1927), and three Gram-negative bacteria, *Escherichia coli* (KCTC 2441), *Salmonella enterica* serovar Typhimurium (KCTC 2515), and *Klebsiella pneumoniae* (KCTC 2690). However, none of the compounds exhibited significant activity against standard bacteria.

Table 3. Growth inhibition 50% (GI_{50}, μM) values of compounds **1–5** against solid cancer cell lines.

Cell Lines Compounds	ACHN	MDA-MB-231	PC-3	NUGC-3	NCI-H23	HCT-15	MRC-9
1	>30	>30	>30	>30	>30	>30	>30
2	>30	>30	>30	>30	>30	>30	>30
3	>30	>30	>30	>30	>30	>30	>30
4	4.58	5.73	6.50	4.34	5.13	5.73	7.23
5	>30	>30	>30	>30	>30	>30	>30
Adriamycin	0.222	0.210	0.106	0.245	0.221	0.305	0.314

Adriamycin is used as a positive control.

3. Materials and Methods

3.1. General Experimental Procedures

One-dimensional and two-dimensional NMR data were obtained using a Bruker 600 MHz spectrometer (Bruker BioSpin GmbH, Rheinstetten, Germany). High-resolution ESIMS data were acquired with a Sciex X500R Q-TOF spectrometer (Sciex, Framingham, MA, USA). Low-resolution ESIMS data were obtained using an ISQEM mass spectrometer (Thermo Fisher Scientific, Waltham, MA, USA). UV–VIS spectra were measured with a Thermoscientific GENESYS 180 spectrophotometer (Thermo Fisher Scientific, Waltham, MA, USA). IR spectra were recorded using a JASCO FT/IR-4100 spectrophotometer (JASCO Corporation, Tokyo, Japan). Optical rotation values were measured with a Rudolph analytical Autopol III S2 polarimeter with a sodium D line at 589 nm and a 10 mm path length (Rudolph Research Analytical, Hackettstown, NJ, USA). HPLC experiments were performed using a BLS-Class pump (Teledyne SSI, Inc., State College, PA, USA) on an ODS column (YMC-Pack-ODS-A, 250 × 10 mm i.d, 5 μm, Kyoto, Japan) with a Shodex RI-201H refractive index detector (Shoko Scientific Co., Ltd., Yokohama, Japan).

3.2. Isolation and Identification of the Strain 238DD-017

The strain 238DD-017 was isolated from a sediment sample collected off-shore of Dokdo, Republic of Korea, during expeditions in August 2023. Aboard the ship, the sediment was collected by a piston corer, and the sample was put into sterile 50 mL conical tubes and stored at 5 °C for transport to the laboratory. Then, to eliminate unwanted microorganisms, heating pretreatment was performed. Each 1 g of sediment sample was placed on a sterile plate and kept in an oven at 60 °C for 30 min. After the heating pretreatment, 0.1 g of sediment was serially diluted to 10^{-1}, 10^{-2}, and 10^{-3} by sterile seawater, and each diluent (50 μL) was spread on humic acid vitamin (HV) agar, actinomycetes isolation agar (AIA), and on Bennett's (BN) agar media. The agar plates were incubated in a BOD (Bio-Oxygen Demand) incubator at 28 °C for 7~28 days until colonies appeared. After incubation, the selected colonies were transferred onto new BN agar plates and purification was performed several times until single pure colonies were visible. The strain 238DD-017 was isolated from the HV agar and incubated for 7 days. The strain was identified as *Actinomadura geliboluensis* based on 16S rRNA gene sequence analysis by Macrogen Inc. (Seoul, Republic of Korea). The sequence of 238DD-017 was registered in GenBank (GenBank accession number PQ312698).

3.3. Fermentation of the Strain 238DD-017

The seed and mass cultures of the strain 238DD-017 were carried out using a BN medium (glucose 10 g, tryptone 2 g, yeast extract 1 g, beef extract 1 g, glycerol 5 g, and sea salt 32 g/L). A single colony of the strain from an agar plate was aseptically inoculated into a 100 mL conical flask filled with 50 mL of BN broth medium and incubated at 28 °C for 14 days on a rotary shaker at 140 rpm. The broth culture (50 mL) was aseptically transferred to a 2 L flask containing 1 L of BN broth, and the strain was incubated at 28 °C for 14 days on a rotary shaker at 120 rpm. The seed culture broth was inoculated into a 100 L fermenter filled with 70 L of BN broth and incubated at 28 °C for 14 days.

3.4. Extraction and Isolation of Metabolites

The mass culture broth (70 L) was harvested and separated into supernatant and mycelium by centrifugation at 60,000 rpm. The supernatant was extracted twice with an equal volume of ethyl acetate (EtOAc, 70 L × 2) and the EtOAc layer was evaporated to yield a crude extract (8.8 g). The crude extract was loaded into ODS column chromatography followed by a stepwise gradient elution with methanol (MeOH) in H_2O (1:4, 2:3, 3:2, 4:1,

and 10:0, *v*/*v*). The fraction eluted with MeOH/H$_2$O (4:1, 92.3 mg) was purified by a semi-preparative reversed-phase HPLC (YMC-Pack-ODS-A, 250 × 10 mm i.d, 5 μm; flow rate: 2.0 mL/min; detector: RI) using isocratic elutions of 65% MeOH in H$_2$O to yield compound **1** (3.8 mg, t_R = 28 min) and 70% MeOH in H$_2$O to yield compounds **2** (1.0 mg, t_R = 42 min), **3** (1.5 mg, t_R = 40 min), and **4** (1.0 mg, t_R = 34 min). The fraction eluted with MeOH/H$_2$O (10:0, 438.1 mg) was purified by a semi-preparative reversed-phase HPLC (YMC-Pack-ODS-A, 250 × 10 mm i.d, 5 μm; flow rate: 2.0 mL/min; detector: RI) using an isocratic elution of 85% MeOH in H$_2$O to yield compound **5** (1.9 mg, t_R = 19 min).

Geliboluol A (**1**): a reddish powder; $[\alpha]_D^{25}$ +37.8 (*c* 0.1, MeOH); UV (MeOH) λ_{max} (log ε) 210 (3.08) nm; IR ν_{max} 3491, 2948, 1056 cm^{-1}; HRESIMS *m*/*z* 343.2239, [M + Na]$^+$, calcd for C$_{20}$H$_{32}$O$_3$Na 343.2244. For ^{1}H NMR (CD$_3$OD, 600 MHz), see Table 1. For ^{13}C NMR (CD$_3$OD, 150 MHz), see Table 1.

Geliboluol B (**2**): a white powder; $[\alpha]_D^{25}$ +29.9 (*c* 0.1, MeOH); UV (MeOH) λ_{max} (log ε) 209 (3.00) nm; IR ν_{max} 3498, 2924, 1015 cm^{-1}; HRESIMS *m*/*z* 319.2273, [M-H]$^-$, calcd for C$_{20}$H$_{31}$O$_3$ 319.2279. For ^{1}H NMR (CD$_3$OD, 600 MHz), see Table 1. For ^{13}C NMR (CD$_3$OD, 150 MHz), see Table 1.

Geliboluol C (**3**): a white solid; $[\alpha]_D^{25}$ +43.5 (*c* 0.1, MeOH); UV (MeOH) λ_{max} (log ε) 210 (3.08) nm; IR ν_{max} 3396, 1043 cm^{-1}; HRESIMS *m*/*z* 343.2229, [M + Na]$^+$, calcd for C$_{20}$H$_{32}$O$_3$Na 343.2227. For ^{1}H NMR (CD$_3$OD, 600 MHz), see Table 1. For ^{13}C NMR (CD$_3$OD, 150 MHz), see Table 1.

Geliboluol D (**4**): a white powder; $[\alpha]_D^{25}$ +59.9 (*c* 0.1, MeOH); UV (MeOH) λ_{max} (log ε) 209 (2.88) nm; IR ν_{max} 2898, 1049 cm^{-1}; HRESIMS *m*/*z* 359.2187, [M + Na]$^+$, calcd for C$_{20}$H$_{32}$O$_4$Na 359.2193. For ^{1}H NMR (CD$_3$OD, 600 MHz), see Table 1. For ^{13}C NMR (CD$_3$OD, 150 MHz), see Table 1.

Compound **5**: a white powder; $[\alpha]_D^{25}$ +63.2 (*c* 0.1, MeOH); UV (MeOH) λ_{max} (log ε) 208 (3.04) nm; IR ν_{max} 3610, 2911 cm^{-1}; LRESIMS *m*/*z* 287.30, [M − H$_2$O + H]$^+$, see Figure S36. For ^{1}H NMR (CD$_3$OD, 600 MHz), see Figure S37. For ^{13}C NMR (CD$_3$OD, 150 MHz), see Figure S38.

3.5. Preparation of MPA Esters of Compound *1*

(*R*)-α-methoxyphenylacetic acid (MPA) (2.5 mg), *N*,*N'*-dicyclohexylcarbodiimide (DCC) (1.5 mg), and 4-dimethylaminopyridine (DMAP) (0.8 mg) were added to a solution of compound **1** (0.3 mg) in methylene chloride (1.0 mL) to obtain the (*R*)-MPA ester of compound **1** (**1a**). The mixture was stirred at room temperature for 72 h. The reaction mixture was then dried under a N$_2$ gas steam at 38 °C and was extracted with EtOAc. The extract was purified by reversed-phase HPLC to obtain **1a**. (*S*)-MPA ester of **1** (**1b**) was also acquired by the same procedure with (*S*)-α-methoxyphenylacetic acid (MPA). NMR data were measured in CD$_3$OD.

(*R*)-MPA ester of **1** (**1a**): δ_H 7.45-7.35 (MPA-Ar), 4.85 (MPA-H), 4.77, 4.73 (H-17), 4.42 (H-3), 4.31 (H-6), 3.40 (MPA-OMe), 2.84, 1.69 (H-15), 2.58 (H-13), 2.57, 1.36 (H-14), 2.03, 1.32 (H-11), 1.91, 1.32 (H-7), 1.89, 1.34 (H-1), 1.78, 1.55 (H-12), 1.61, 1.41 (H-2), 1.48 (H-20), 1.43 (H-5), 1.24 (H-19), and 0.91 (H-18).

(*S*)-MPA ester of **1** (**1b**): δ_H 7.44-7.33 (MPA-Ar), 4.83 (MPA-H), 4.77, 4.72 (H-17), 4.37 (H-3), 4.20 (H-6), 3.38 (MPA-OMe), 2.83, 1.67 (H-15), 2.57 (H-13), 2.55, 1.34 (H-14), 1.94, 1.32 (H-11), 1.97, 1.27 (H-7), 1.91, 1.40 (H-1), 1.78, 1.54 (H-12), 1.81, 1.64 (H-2), 1.51 (H-20), 1.35 (H-5), 1.09 (H-19), and 0.46 (H-18).

3.6. CellTiter-Glo (CTG) and Sulforhodamine B (SRB) Assay for Cytotoxicity Testing

The cytotoxicity test was conducted with CTG luminescent cell viability and SRB assay according to the published procedures [34,35]. Briefly, blood cancer cell lines and a normal

cell line were obtained from the American Type Culture Collection (Manassas, VA, USA) (HL-60: acute myelogenous leukemia, Raji: Burkitt's lymphoma, NALM6 C. G5: B-cell acute lymphocytic leukemia, K562: chronic myelogenous leukemia, U266: multiple myeloma, and RPMI-1788: B lymphocytes) and the DSMZ-German Collection of Microorganisms and Cell Cultures (WSU-DLCL2: diffuse large B-cell lymphoma and RPMI-8402: T-cell acute lymphocytic leukemia). The cell lines were incubated in RPMI 1640 supplemented with 10% fetal bovine serum, penicillin (100 IU/mL), and streptomycin (100 μg/mL) at 37 °C under a humidified atmosphere of 5% CO_2. The cells with a passage number between 8 and 12 were used. The cell lines were prepared in an opaque-walled 96-well plate (8×10^3 cells/well), and the compounds (**1–5** and doxorubicin as a positive control) with 0.1% DMSO were added to each well and incubated for 48 h. The cell cultures were then treated with 100 μL of CellTiter-Glo Reagent (Promega, Madison, WI, USA) and kept for 10 min to acquire a luminescence signal. Luminescence measurements were performed with the GloMax-Multi Detection System (Promega, Madison, WI, USA). The solid cancer cell lines and the normal cell line were obtained from the American Type Culture Collection (Manassas, VA, USA) (ACHN: renal, MDA-MB-231: breast, PC-3: prostate, NCI-H23: lung, HCT-15: colon, and MRC-9: lung fibroblast) and the Japanese Cancer Research Resources Bank (JCRB) (NUGC-3: stomach). The cell lines were incubated in RPMI 1640 supplemented with 10% fetal bovine serum, penicillin (100 IU/mL), and streptomycin (100 μg/mL) at 37 °C under a humidified atmosphere of 5% CO_2. The cells with a passage number between 8 and 12 were used. The cells were then prepared in a 96-well plate (8×10^3 cells/well), and the compounds (**1–5** and adriamycin as a positive control) with 0.1% DMSO were added to each well. After incubation for 48 h, the cell cultures were fixed using 50% trichloroacetic acid (50 μg/mL) and were dyed with 0.4% SRB in 1% acetic acid. Unbound dye was washed using 1% acetic acid and protein-bound dye was collected with 10 mM Tris base (pH 10.5) to measure optical density. Absorbance was measured at 540 nm with a VersaMax microplate reader (Molecular Devices, Sunnyvale, CA, USA) and GI_{50} values were calculated by GraphPad Prism 4.0 (GraphPad, San Diego, CA, USA).

4. Conclusions

In conclusion, five kaurane-type diterpenoids were isolated from the rare actinomycete *Actinomadura geliboluensis* 238DD-017, including four new compounds (**1–4**), namely, geliboluols A–D. The structures of the new compounds **1–4** were determined by a detailed analysis of the HR-ESIMS and NMR data, and as a result, compounds **1–4** were confirmed as kaurane-type diterpenoids, which are uncommon in nature. Compounds **1–5** were evaluated for their cytotoxicity. Compounds **4** and **5** showed cytotoxicity against seven blood cancer cell lines with GI_{50} values ranging from 2.59 to 22.50 μM, while against the six solid cancer cell lines, only **4** displayed cytotoxicity, with GI_{50} values ranging from 4.34 to 7.23 μM. These results expand the field of kaurane-type diterpenoids research of the genus *Actinomadura*.

Supplementary Materials: The following supporting information can be downloaded at: https://www.mdpi.com/article/10.3390/md23020078/s1. Figures S1–S35: ^{1}H, ^{13}C, and 2D NMR spectra (COSY, HSQC, HMBC, and NOESY), and HRESIMS data of compounds **1–4**. Figures S36–S38: ^{1}H, ^{13}C NMR, and LR-MS data of compound **5**. Table S1: Cytotoxicity test results of compounds **1–5**.

Author Contributions: Conceptualization, H.J.S.; investigation, C.-S.H., J.S.K. and J.-W.Y.; resources, M.A.L., H.-S.L. and C.H.K.; writing—original draft preparation, C.-S.H.; writing—review and editing, H.J.S.; project administration, H.J.S.; funding acquisition, H.J.S. All authors have read and agreed to the published version of the manuscript.

Institutional Review Board Statement: Not applicable.

Informed Consent Statement: Not applicable.

Data Availability Statement: The data presented in this article are available in the Supplementary Materials.

Conflicts of Interest: The authors declare no conflicts of interest.

References

1. Ambrosio, S.R.; Tirapelli, C.R.; da Costa, F.B.; de Oliveira, A.M. Kaurane and pimarane-type diterpenes from the *Viguiera* species inhibit vascular smooth muscle contractility. *Life Sci.* **2006**, *79*, 925–933. [CrossRef] [PubMed]

2. García, P.A.; de Oliveira, A.B.; Batista, R. Occurrence, biological activities and synthesis of kaurane diterpenes and their glycosides. *Molecules* **2007**, *12*, 455–483. [CrossRef]

3. Zhao, X.; Cacherat, B.; Hu, Q.; Ma, D. Recent advances in the synthesis of *ent*-kaurane diterpenoids. *Nat. Prod. Rep.* **2022**, *39*, 119–138. [CrossRef]

4. Ibrahim, T.S.; Khongorzul, P.; Muyaba, M.; Alolga, R.N. *Ent*-kaurane diterpenoids from the Annonaceae family: A review of research progress and call for further research. *Front. Pharmacol.* **2023**, *14*, 1227574. [CrossRef] [PubMed]

5. Antoine, G.; Vaissayre, V.; Meile, J.C.; Payet, J.; Conéjéro, G.; Costet, L.; Fock-Bastide, I.; Joët, T.; Dussert, S. Diterpenes of *Coffea* seeds show antifungal and anti-insect activities and are transferred from the endosperm to the seedling after germination. *Plant Physiol. Biochem.* **2023**, *194*, 627–637. [CrossRef] [PubMed]

6. Schmelz, E.A.; Huffaker, A.; Sims, J.W.; Christensen, S.A.; Lu, X.; Okada, K.; Peters, R.J. Biosynthesis, elicitation and roles of monocot terpenoid phytoalexins. *Plant J.* **2014**, *79*, 659–678. [CrossRef] [PubMed]

7. Herrera-Acevedo, C.; Flores-Gaspar, A.; Scotti, L.; Mendonça-Junior, F.J.B.; Scotti, M.T.; Coy-Barrera, E. Identification of Kaurane-Type Diterpenes as Inhibitors of Leishmania Pteridine Reductase I. *Molecules* **2021**, *26*, 3076. [CrossRef]

8. Qu, J.-B.; Zhu, R.-L.; Zhang, Y.-L.; Guo, H.-F.; Wang, X.-N.; Xie, C.-F.; Yu, W.-T.; Ji, M.; Lou, H.-X. *ent*-Kaurane Diterpenoids from the Liverwort *Jungermannia atrobrunnea*. *J. Nat. Prod.* **2008**, *71*, 1418–1422. [CrossRef] [PubMed]

9. Zhou, Z.-S.; Wang, Z.-J.; Tian, B.; Zhu, Y.-Y.; Wei, M.-Z.; Zhao, Y.-L.; Luo, X.-D. Three New *Ent*-Kaurane Diterpenes with Antibacterial Activity from *Sigesbeckia orientalis*. *Molecules* **2024**, *29*, 4631. [CrossRef]

10. Hai, Q.X.; Hu, K.; Chen, S.P.; Fu, Y.Y.; Li, X.N.; Sun, H.D.; He, H.P.; Puno, P.T. Silvaticusins A-D: *Ent*-kaurane diterpenoids and a cyclobutane-containing *ent*-kaurane dimer from *Isodon silvaticus*. *Nat. Prod. Bioprospect.* **2024**, *14*, 45. [CrossRef]

11. Xing, H.; An, L.; Song, Z.; Li, S.; Wang, H.; Wang, C.; Zhang, J.; Tuerhong, M.; Abudukeremu, M.; Li, D.; et al. Anti-Inflammatory *ent*-Kaurane Diterpenoids from *Isodon serra*. *J. Nat. Prod.* **2020**, *83*, 2844–2853. [CrossRef] [PubMed]

12. Wu, Y.-C.; Hung, Y.-C.; Chang, F.-R.; Cosentino, M.; Wang, H.-K.; Lee, K.-H. Identification of *ent*-16β,17-Dihydroxykauran-19-oic Acid as an Anti-HIV Principle and Isolation of the New Diterpenoids Annosquamosins A and B from *Annona squamosa*. *J. Nat. Prod.* **1996**, *59*, 635–637. [CrossRef]

13. Schniete, J.K.; Fernández-Martínez, L.T. Natural product discovery in soil actinomycetes: Unlocking their potential within an ecological context. *Curr. Opin. Microbio.* **2024**, *79*, 102487. [CrossRef]

14. Law, J.W.-F.; Law, L.N.-S.; Letchumanan, V.; Tan, L.T.-H.; Wong, S.H.; Chan, K.-G.; Ab Mutalib, N.-S.; Lee, L.-H. Anticancer Drug Discovery from Microbial Sources: The Unique Mangrove Streptomycetes. *Molecules* **2020**, *25*, 5365. [CrossRef]

15. Jensen, P.R.; Moore, B.S.; Fenical, W. The marine actinomycete genus *Salinispora*: A model organism for secondary metabolite discovery. *Nat. Prod. Rep.* **2015**, *32*, 738–751. [CrossRef] [PubMed]

16. Dashti, Y.; Errington, J. Chemistry and biology of specialized metabolites produced by *Actinomadura*. *Nat. Prod. Rep.* **2024**, *41*, 370–401. [CrossRef]

17. Shin, B.; Kim, B.Y.; Cho, E.; Oh, K.B.; Shin, J.; Goodfellow, M.; Oh, D.C. Actinomadurol, an Antibacterial Norditerpenoid from a Rare Actinomycete, *Actinomadura* sp. KC 191. *J. Nat. Prod.* **2016**, *79*, 1886–1890. [CrossRef] [PubMed]

18. Wang, Y.; Zhang, L.; Wei, Y.; Huang, W.; Li, L.; Wu, A.-A.; Dastur, A.; Greninger, P.; Bray, W.M.; Zhang, C.-S.; et al. Pharmacological Targeting of Vacuolar H+-ATPase via Subunit V1G Combats Multidrug-Resistant Cancer. *Cell Chem. Biol.* **2020**, *27*, 1359–1370. [CrossRef]

19. Kusserow, K.; Gulder, T.A.M. Complete Genome Sequence of *Actinomadura parvosata* subsp. kistnae, a rich source of novel natural product (bio-) chemistry. *J. Genom.* **2017**, *5*, 75–76.

20. Saricaoglu, S.; Saygin, H.; Topkara, A.R.; Gencbay, T.; Guven, K.; Cetin, D.; Sahin, N.; Isik, K. *Actinomadura soli* sp. nov., isolated from the top soil layer on basaltic material in Turkey. *Int. J. Syst. Evol. Microbiol.* **2021**, *71*, 005062. [CrossRef]

21. Ay, H. Genomic insight into a novel actinobacterium, *Actinomadura rubrisoli* sp. nov., reveals high potential for bioactive metabolites. *Antonie Leeuwenhoek* **2021**, *114*, 195–208. [CrossRef]

22. Parra, J.; Beaton, A.; Seipke, R.F.; Wilkinson, B.; Hutchings, M.I.; Duncan, K.R. Antibiotics from rare actinomycetes, beyond the genus *Streptomyces*. *Curr. Opin. Microbiol.* **2023**, *76*, 102385. [CrossRef]

23. Sazak, A.; Camas, M.; Spröer, C.; Klenk, H.P.; Sahin, N. *Actinomadura geliboluensis* sp. nov., isolated from soil. *Int. J. Syst. Evol. Microbiol.* **2012**, *62*, 2011–2017. [CrossRef] [PubMed]

24. Zhang, Z.; Zhou, T.; Yang, T.; Fukaya, K.; Harunari, E.; Saito, S.; Yamada, K.; Imada, C.; Urabe, D.; Igarashi, Y. Nomimicins B-D, new tetronate-class polyketides from a marine-derived actinomycete of the genus *Actinomadura*. *Beilstein J. Org. Chem.* **2021**, *17*, 2194–2202. [CrossRef]

25. Kuo, P.-C.; Shen, Y.-C.; Yang, M.-L.; Wang, S.-H.; Thang, T.D.; Dung, N.X.; Chiang, P.-C.; Lee, K.-H.; Lee, E.J.; Wu, T.-S. Crotonkinins A and B and Related Diterpenoids from *Croton tonkinensis* as Anti-inflammatory and Antitumor Agents. *J. Nat. Prod.* **2007**, *70*, 1906–1909. [CrossRef] [PubMed]

26. Lorimer, S.D.; Weavers, R.T. Foliage sesquiterpenes and diterpenes of *Podocarpus spicatus*. *Phytochemistry* **1987**, *26*, 3207–3215. [CrossRef]

27. Qi, X.-L.; Zhang, Y.-Y.; Zhao, P.; Zhou, L.; Wang, X.-B.; Huang, X.-X.; Lin, B.; Song, S.-J. *ent*-Kaurane Diterpenoids with Neuroprotective Properties from Corn Silk (*Zea mays*). *J. Nat. Prod.* **2018**, *81*, 1225–1234. [CrossRef] [PubMed]

28. Chen, X.; Wu, X.; Ouyang, W.; Gu, M.; Gao, Z.; Song, M.; Chen, Y.; Lin, Y.; Cao, Y.; Xiao, H. Novel *ent*-Kaurane Diterpenoid from Rubus *corchorifolius* L. f. Inhibits Human Colon Cancer Cell Growth via Inducing Cell Cycle Arrest and Apoptosis. *J. Agric. Food Chem.* **2017**, *65*, 1566–1573. [CrossRef] [PubMed]

29. Ren, H.; Xu, Q.-L.; Luo, Y.; Zhang, M.; Zhou, Z.-Y.; Dong, L.-M.; Tan, J.-W. Two new *ent*-kaurane diterpenoids from *Wedelia trilobata* (L.) Hitchc. *Phytochem. Lett.* **2015**, *11*, 260–263. [CrossRef]

30. Wu, H.-Y.; Zhan, R.; Wang, W.-G.; Jiang, H.-Y.; Du, X.; Li, X.-N.; Li, Y.; Pu, J.-X.; Sun, H.-D. Cytotoxic *ent*-Kaurane Diterpenoids from *Isodon wikstroemioides*. *J. Nat. Prod.* **2014**, *77*, 931–941. [CrossRef] [PubMed]

31. Riehl, P.S.; DePorre, Y.C.; Armaly, A.M.; Groso, E.J.; Schindler, C.S. New avenues for the synthesis of *ent*-kaurene diterpenoids. *Tetrahedron* **2015**, *71*, 6629–6650. [CrossRef]

32. Han, Q.B.; Li, M.L.; Li, S.H.; Mou, Y.K.; Lin, Z.W.; Sun, H.D. *Ent*-kaurane diterpenoids from *Isodon rubescens* var. *lushanensis*. *Chem. Pharm. Bull.* **2003**, *51*, 790–793. [CrossRef] [PubMed]

33. CLSI. *Methods for Dilution Antimicrobial Susceptibility Tests for Bacteria that Grow Aerobically*, 11th ed.; CLSI Standard M07; Clinical and Laboratory Standards Institute: Wayne, PA, USA, 2018.

34. Choi, B.-K.; Trinh, P.T.H.; Lee, H.-S.; Choi, B.-W.; Kang, J.S.; Ngoc, N.T.D.; Van, T.T.T.; Shin, H.J. New Ophiobolin Derivatives from the Marine Fungus *Aspergillus flocculosus* and Their Cytotoxicities against Cancer Cells. *Mar. Drugs* **2019**, *17*, 346. [CrossRef] [PubMed]

35. Lee, E.; Cho, H.; Lee, D.K.; Ha, J.; Choi, B.J.; Jeong, J.H.; Ryu, J.-H.; Kang, J.S.; Jeon, R. Discovery of 5-Phenoxy-2-aminopyridine Derivatives as Potent and Selective Irreversible Inhibitors of Bruton's Tyrosine Kinase. *Int. J. Mol. Sci.* **2020**, *21*, 8006. [CrossRef] [PubMed]